ELSEVIER

Available online at www.sciencedirect.com

SCIENCE DIRECT®

Journal of Crystal Growth 284 (2005) 379–387

JOURNAL OF CRYSTAL GROWTH

www.elsevier.com/locate/jcrysgro

Growth and characterization of cubic $In_xGa_{1-x}N$ epilayers on two different types of substrate

D.G. Pacheco-Salazar[a], S.F. Li[b], F. Cerdeira[c], E.A. Meneses[c,*], J.R. Leite[a,†], L.M.R. Scolfaro[a], D.J. As[b], K. Lischka[b]

[a]*Instituto de Física, Universidade de São Paulo, P.O. Box 66318, São Paulo-SP, Brazil*
[b]*University of Paderborn, Department of Physics, Warburger Str. 100, D-33098 Paderborn, Germany*
[c]*Instituto de Física Gleb Wataghin, Universidade Estadual de Campinas, P.O. Box 6165, Campinas-SP, Brazil*

Received 9 May 2005; received in revised form 15 June 2005; accepted 29 July 2005

Communicated by R.M. Biefeld

Abstract

We report on the growth and characterization of cubic InGaN epilayers on two different types of substrates: GaAs (0 0 1) and 3C-SiC (0 0 1). The films are grown by RF plasma-assisted molecular beam epitaxy (MBE). The crystalline quality and state of stress in these films were assessed by performing Raman scattering and X-ray diffraction experiments. Both types of measurements complement one another as techniques to determine crystalline quality and the state of biaxial strain present in the alloy layers. Our experiments show that, for the same In molar fraction, samples deposited on SiC substrates are more uniformly strained and have better crystallinity than those deposited on GaAs substrates.

© 2005 Elsevier B.V. All rights reserved.

PACS: 81.15.Hi; 81.05.Ea; 78.55.Cr; 78.66.Fd; 78.67.Hc

Keywords: A1. Crystalline quality; A1. Raman scattering; A1. X-ray diffraction

1. Introduction

Low cost short-haul communication systems using polymethyl methacrylate (PMMA) plastic optical fibers (POFs) require inexpensive light sources emitting around the PMMA absorption minimum at 510 nm (around 70 dB/km). For the realization of these devices group III-nitride wide-band-gap semiconductors are the material of choice. Due to their large direct band-gap they are well suited for a wide range of applications, e.g. as light emitter in the green to ultraviolet range

*Corresponding author. Tel.: +55 19 37885467; fax: +55 37884146.
E-mail address: eliermes@ifi.unicamp.br (E.A. Meneses).
†Deceased.

0022-0248/$ - see front matter © 2005 Elsevier B.V. All rights reserved.
doi:10.1016/j.jcrysgro.2005.07.049

or as detectors [1]. Group III-nitrides can be produced in the thermodynamic stable configuration with hexagonal (wurtzite) crystal structure and in a metastable modification with cubic (zincblende) structure. The main difference between these two modifications is the absence of piezoelectric and spontaneous polarization fields in the cubic modification [2]. Furthermore, due to the slightly smaller energy gap of the cubic nitrides (200 meV lower than their hexagonal counterpart), smaller mol fractions of In in the well of InGaN/GaN quantum wells are necessary to reach emission wavelengths beyond 510 nm. Therefore, group III-nitrides seem to be the material of choice for the realization of resonant cavity light emitting diodes (RC-LED) for the 500–570 nm spectral range [3]. Hence, the growth of cubic InGaN layers is of great importance, as is the appropriate characterization of the ultimate crystalline quality achieved in these layers.

In this work we report on the growth and characterization of InGaN layers on two different types of substrates: (0 0 1) GaAs and (0 0 1) 3C-SiC. The latter consists of a film of approximately 200 μm grown on a (0 0 1) Si wafer. In both cases a thick (~500 nm) GaN buffer layer is deposited first and on this buffer the InGaN layer is grown. The films are grown by RF plasma-assisted molecular beam epitaxy (MBE). Since the lattice mismatch [4–6] between GaN and GaAs (~20%) is much larger than that between GaN and 3C-SiC (~3.6%), we would expect better pseudomorphic growth on the latter. In order to test this idea, we performed Raman scattering and X-ray diffraction (XRD) experiments on these epilayers. In what follows, we describe the use of both techniques to systematically evaluate the crystalline quality of the films grown on each of these two substrates. Both types of measurements complement one another as techniques to determine crystalline order and the state of biaxial strain present in the alloy layers. Our experiments show that, for the same In molar fraction, samples deposited on SiC substrates tend to be more uniformly strained and have better crystallinity than those deposited on GaAs substrates.

2. Experiment

Cubic $In_xGa_{1-x}N$ epilayers were grown by plasma-assisted MBE on two different types of substrates. One of these substrates consisted of about 200 μm thick 3C-SiC (0 0 1). A commercial Riber 32 MBE system equipped with an Oxford Applied Research HD 25 radio frequency N-plasma source was used. Conventional Knudsen cells were used for the evaporation of In and Ga. After cleaning of the 3C-SiC substrates a thick cubic GaN buffer layer (about 500 nm) was grown at 720 °C [7]. After a growth interruption for reducing the substrate temperature, about 50 nm thick $In_xGa_{1-x}N$ epilayers were grown at 620 °C. By adjusting the In to Ga flux ratio, the In content was varied between $x = 0.028$ and 0.171. The second substrate consisted of GaAs (0 0 1) wafers. The procedure to grow the InGaN layer on this substrate was very similar to that on the SiC substrate. Before starting the InGaN growth on the GaAs substrates, a GaN buffer layer (~700 nm thick) was grown at a substrate temperature of about 720 °C. This growth was performed under slightly Ga-rich conditions. For the growth of the InGaN layer the temperature of the substrate was decreased to 620–630 °C. This procedure is described in detail in Ref. [8]. The characteristics of the samples used in our experiments are summarized in Table 1. The cubic nature, the phase purity and the crystalline quality of the cubic group III-nitrides were verified by high resolution X-ray diffraction (HRXRD), by transmission electron microscopy (TEM) and Raman measurements as explained in detail in Ref. [9].

The In-content and the strain status of the $In_xGa_{1-x}N$ films were measured by high resolution XRD. XRD measurements were performed on a Philips X'pert Materials Research diffractometer. Two types of experiments were performed: ω–2θ scan and ω-scan (rocking curve). Repetitions of the former results in reciprocal space maps (RSM). The combination of these two types of experiments allow the determination of both the In molar fraction (x) and the state of strain of the film. In particular, RSM of the asymmetric $(\bar{1}\,\bar{1}\,3)$ reflection revealed that the thick GaN buffer layers deposited on the 3C-SiC substrates were totally

Table 1
Description of the cubic $In_xGa_{1-x}N$ epilayers and the GaN buffer layer

Samples	Substrate	Indium molar fraction (x)	Thickness in nm of InGaN/GaN	State of strain (Raman)	State of strain (XRD)	ω-scan FWHM (arcmin)
A5	GaAs	0.160	132/823	Totally relaxed	Totally relaxed	41.80
A4	GaAs	0.102	125/695	Partially relaxed	Partially relaxed	62.40
A3	GaAs	0.090	125/725	Partially relaxed	Partially relaxed	57.40
A2	GaAs	0.050	153/615	Partially relaxed	Partially relaxed	48.90
A1	GaAs	0.025	100/625	Not measured	Not measured	50.00
B5	SiC	0.171	55/540	Partially relaxed	Fully strained	23.98
B4	SiC	0.130	51/538	Fully strained	Fully strained	29.50
B3	SiC	0.098	40/390	Fully strained	Fully strained	29.10
B2	SiC	0.065	40/439	Not measured	Fully strained	21.40
B1	SiC	0.028	40/525	Not measured	Fully strained	22.00

The last column lists data corresponding to the GaN layer.

relaxed, whereas all $In_xGa_{1-x}N$ epilayers, deposited on the GaN buffer, appeared to be fully strained.

Unpolarized micro-Raman measurements were made in the backscattering configuration at room temperature using Argon-ion laser excitation (488-nm line) at $\sim 1.5\times10^4\,W/cm^2$. Scattered light was analyzed with a triple Jobin Yvon T-4000 XY spectrometer equipped with a multichannel charge-coupled device. An optical microscope with a $\times 100$ objective was used to focus the laser beam on the sample and collect the scattered light. The laser spot on the sample had a diameter between 1 and 2 μm. The spectral resolution of the system is estimated to be of the order of $1.5\,cm^{-1}$.

3. Results and discussion

3.1. X-ray diffraction measurements

The c-$In_xGa_{1-x}N$/GaN/SiC and c-$In_xGa_{1-x}N$/GaN/GaAs samples were characterized by high-resolution XRD. Figs. 1(a) and (b) show, in a linear intensity scale, ω–2θ spectra for the (0 0 2) reflection of all our samples. Spectra were fitted by *pseudo-Voigt* functions in order to obtain the angular positions of both the GaN and c-$In_xGa_{1-x}N$ peaks. The peak at $\omega\approx19.92^\circ$ originates in the GaN buffer layer, while the peaks at lower angles correspond to the alloy layer. For some samples the latter peak is hard to observe in a linear scale. For this reason, the inset in these figures show data for some samples displayed in a logarithmic vertical scale, where the shoulder corresponding to the alloy peak can be easily distinguished from the stronger GaN peak. These spectra give the lattice plane spacing along the growth direction. This information is not enough to determine the In molar fraction, because this spacing varies with In composition and strain. Also the line width in ω–2θ scans cannot be directly related to crystalline quality, because inhomogeneities in the In molar fraction will also broaden the lines. Hence, a complementary measurement is needed.

One such complementary measurement is provided by ω-scans (rocking curves). The linewidths in this type of scan gives an idea about the parallelism of crystalline grains on the sample surface and can furnish information on crystalline quality [10,11], with smaller linewidths corresponding to better crystallinity. In the last column of Table 1 we list the values of the full-width at half-maximum (FWHM) of the rocking curves of the GaN buffer layer in our samples. For samples grown on GaAs substrates, linewidths vary between 41.8 and 62.4 arcmin, while for those grown on SiC substrates the FWHMs lie between 21.4 and 29.5 arcmin. Hence, this type of measurement indicates that GaN layers grown on SiC have better crystalline quality than those grown on

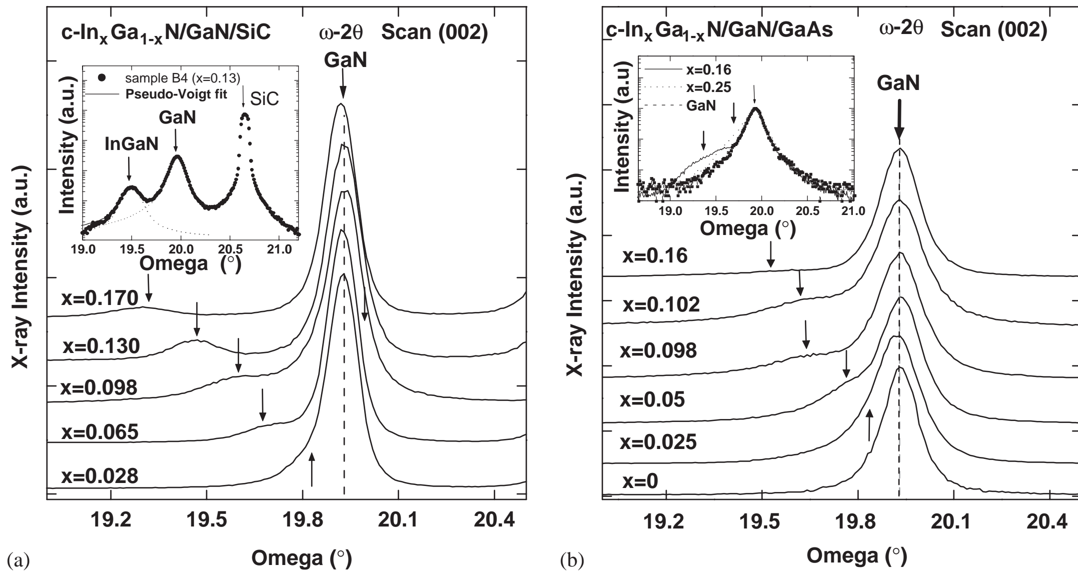

Fig. 1. ω–2θ scans for (0 0 2) reflections. The strongest peak corresponds to the GaN buffer layer while the smaller one originates in the InGaN layers. Here (a) are samples deposited on SiC substrates while (b) are spectra of samples deposited on GaAs substrates.

GaAs. This leads us to believe that the InGaN layers deposited on these buffer layers also have better quality. This can also be inferred from the reciprocal space maps which we discuss next.

Finally, in order to use XRD information to obtain the indium molar fraction of the c-In$_x$Ga$_{1-x}$N/GaN layer, we must refer to the reciprocal space maps. Figs. 2(a) and (b) show representative data of the ($\bar{1}$ $\bar{1}$ 3) reflection for two samples grown on different substrates. In this way, the state of strain of all (but the A$_1$ sample) was determined. The results of these scans are summarized in the last-but-one column of Table 1. The results listed there indicate that all the InGaN films deposited on SiC substrates are fully strained, while those deposited on GaAs substrates are at least partially relaxed. Finally, having the strain information, we used Vegard's rule to determine the In molar fraction. These results are listed in the third column of Table 1. Fig. 2 also indicates that the InGaN layers grown on SiC substrates have better crystalline quality than those grown on GaAs. This is shown by the fact that the width of intensity contours in the Q_x direction is narrower in Fig. 2(a) than in Fig. 2(b).

In the next section we shall discuss the results of performing Raman scattering experiments on the same samples. This technique offers information on sample quality and state of stress which complements the XRD results.

3.2. Raman scattering measurements

Previous studies of Raman scattering from c-In$_x$Ga$_{1-x}$N/GaN layers [11–13] focused their attention on two main subjects: the one or two-mode behavior of the optical phonons of these alloys and the possibility of producing evidence about phase segregation, producing quantum dots of In-rich material within a matrix of an alloy layer of average composition. Here we shall address only the issue of crystallinity and state of tension of the film as inferred from the Raman spectrum. The previous work already established that the alloy exhibits one-mode behavior, i.e.: the Raman spectrum consists of a single TO and a single LO line which vary in frequency linearly between those of the two binary compounds (InN and GaN). The same conclusions can be derived from our spectra. Raman spectra from our samples are displayed in

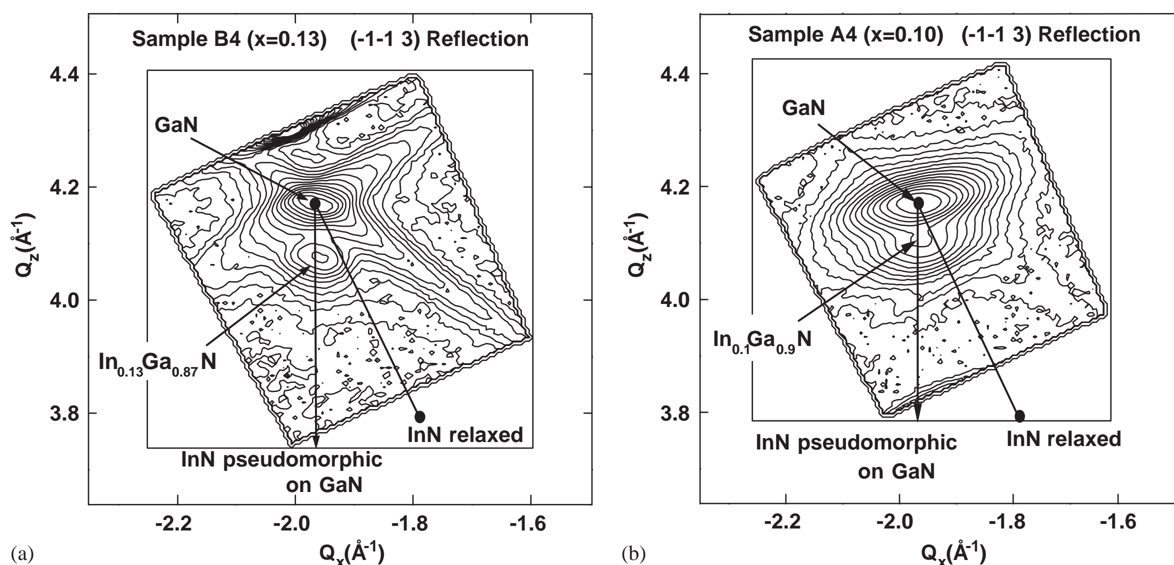

Fig. 2. Reciprocal space maps of (a) $In_xGa_{1-x}N/GaN/SiC$ with $x = 0.13$ and (b) $In_xGa_{1-x}N/GaN/GaAs$ with $x = 0.102$.

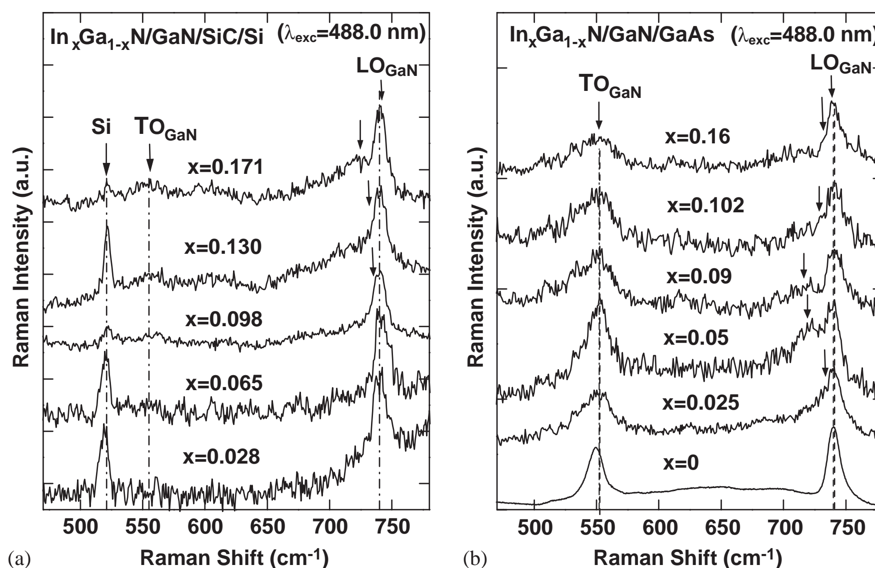

Fig. 3. Raman spectra of (a) $In_xGa_{1-x}N/GaN/SiC$ and (b) $In_xGa_{1-x}N/GaN/GaAs$.

Figs. 3(a) and (b). The spectra show structures originating in both TO (around 550 cm^{-1}) and LO phonons (around 740 cm^{-1}) of the GaN buffer layer and of the alloy. The corresponding lines of the alloy appear as weak shoulders at slightly lower frequencies than the former. This disparity between the intensities of Raman features originating in the alloy and buffer layers is due to the fact that the ratio between the thicknesses of these two layers in our samples is ~0.1 (see Table 1).

Thus, in order to extract information about the frequencies of the alloy phonons a line fitting has to be made of these spectra. Representative examples of these fittings, for samples deposited on both types of substrate, are displayed in Figs. 4(a) and (b). These fittings provide values for both frequencies and relative intensities of all lines. These are the quantities that will be used when trying to extract information about the state of strain of the InGaN layers from these spectra.

First, let us discuss the type of information contained in the relative intensities of the different Raman features. The spectra of Figs. 3 and 4 were taken in the backscattering configuration, with incoming and scattered radiation propagating perpendicularly to the film surface i.e., along the laboratory z-axis. For films of perfect crystalline order, this direction should coincide with the cubic z-axis, the (0 0 1) direction. In such a configuration, scattering by LO phonons is allowed for (x,y) polarization and scattering by TO phonons is strictly forbidden, because it could only occur for (x,z) or (y,z) polarizations, both impossible, because it would require that light be polarized along its propagation direction. However, Fig. 3(b) shows that the line attributed to TO scattering is sometimes as intense as that attributed to LO scattering. This is due to poor crystalline quality. It tells us that, although neither incoming nor scattered radiation can be polarized along the laboratory z-axis, misalignment of crystallites in the film (both in the alloy and the GaN layers) produce grains with the z-axis of the crystallites tilted from the laboratory z-axis. Hence, there can be a projection of the incoming and outgoing beam polarizations along the crystal (0 0 1) direction. If the films were perfect, this would be impossible. Hence, the ratio of the intensity between TO and LO lines (I_{TO}/I_{LO}), which should be zero for a perfect crystal, can be used as an indicator of crystalline quality. A visual inspection of Figs. 3(a) and (b) shows that the (I_{TO}/I_{LO}) ratio is much larger in samples grown on GaAs substrates than in those grown on SiC substrates. In fact, comparing two samples grown on the two types of substrate of approximately the same In molar fraction ($x \approx 0.09$), samples A3 and B3, respectively (see Table 1), we find $(I_{TO}/I_{LO}) = 0.89$ for the sample grown on GaAs and $(I_{TO}/I_{LO}) = 0.19$ for that grown on SiC. These numbers refer to the intensity ratio of the GaN peaks, since those of the alloy TO-phonons from the InGaN films grown on SiC are so weak that they do not show up in our spectra. Thus, the crystalline quality of the GaN buffers grown on

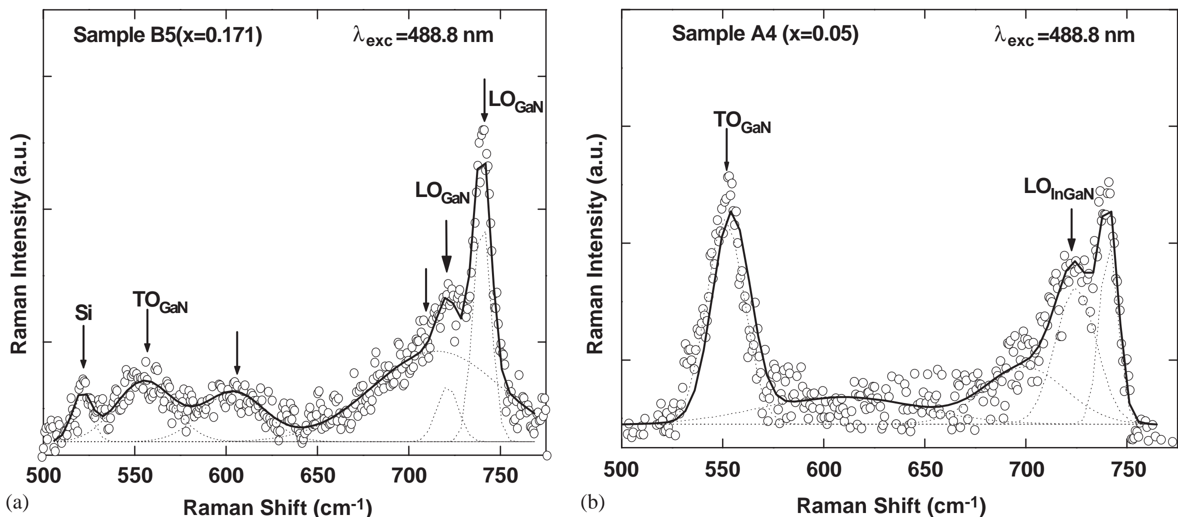

Fig. 4. Fittings of the Raman spectra with Gaussian structures of adjustable positions, linewidth and intensities for (a) $In_xGa_{1-x}N$/GaN/SiC with $x = 0.17$ and (b) $In_xGa_{1-x}N$/GaN/GaAs with $x = 0.05$.

SiC substrates appears to be much better than that grown on GaAs substrates. The alloy layers should follow this trend, as shown by the fact that the TO line from the alloy layer is only visible in the spectra of films grown on GaAs. These results are in agreement with those obtained by analyzing the rocking curves linewidth discussed previously.

Phonon frequencies are affected by the In content of the alloy and by the state of strain of the film. In totally relaxed films the former gives a linear decrease of the phonon frequency as the In molar fraction (x) of the c-$In_xGa_{1-x}N$ increases. We shall focus our attention on the LO phonon, which is the one more clearly observed in the spectra of all our samples (see Figs. 2 and 3). In Fig. 5 we represent this linear tendency for the data of Tabata et al. [11], which corresponds to thick, totally relaxed (unstrained) c-$In_xGa_{1-x}N$ films deposited on a GaN substrate (full squares). The straight line corresponds to a linear least-squares fit to their data and represents the dependence of the LO frequency on In molar fraction for unstrained films. This line is given by

$$\omega^0_{\mathrm{LO}}(x) = \omega^0_{\mathrm{GaN}} - \Gamma x, \quad (1)$$

where $\omega^0_{\mathrm{LO}}(x) = 741.73\,\mathrm{cm}^{-1}$, $\Gamma = 153.29\,\mathrm{cm}^{-1}$ and the superscript "0" signifies absence of strain. The presence of strain can also be represented by a

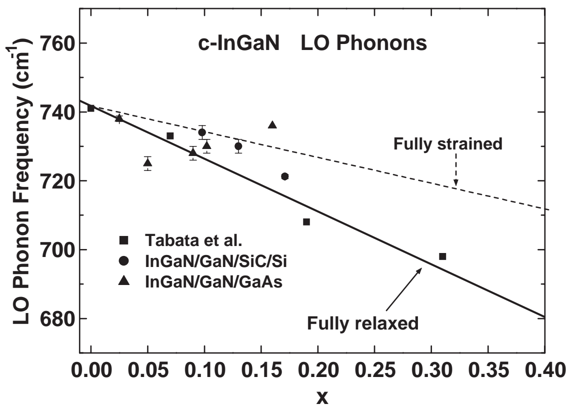

Fig. 5. LO phonon frequencies of $In_xGa_{1-x}N$ layers as a function of Indium molar fraction (x). The solid line is obtained by fitting the data for fully relaxed layers while the dotted line is calculated (see text) for fully strained layers.

linear equation [14–16]:

$$\delta\omega = \omega - \omega_0 = \frac{p}{2\omega_0}\varepsilon_{zz} + \frac{q}{2\omega_0}(\varepsilon_{xx} + \varepsilon_{yy}), \quad (2)$$

where ω (ω_0) is the frequency of the LO phonon in the strained (unstrained) material, $\varepsilon_{i,j}$ are the components of the strain tensor and p and q are deformation potential constants. For biaxial strain, this equation can be re-written as [17]

$$\frac{\delta\omega}{\omega_0} = \frac{2q - \alpha p}{2\omega_0^2}\varepsilon = b\varepsilon \quad (3)$$

with

$$b = \frac{2q - \alpha p}{2\omega_0^2}, \quad \alpha = \frac{2C_{12}}{C_{11}} = \frac{-2S_{12}}{S_{11} + S_{12}} \quad \text{and}$$
$$\varepsilon = \frac{a - a_0}{a_0}. \quad (4)$$

In the above equations, $C_{i,j}$ ($S_{i,j}$) are the elastic stiffness coefficients (compliances) of the strained material and a (a_0) is the in-plane lattice constant of the strained (unstrained buffer) layer. In the case of the c-$In_xGa_{1-x}N$, $a(x)$ can be obtained by using Vegard's rule. Combining all these dependences, and keeping only linear terms in x and ε, we obtain (for a fully strained film)

$$\omega(x) \cong 741.73 - (153.29 - 70.179|b|)x, \quad (5)$$

where frequencies are given in cm^{-1} and both x and b are dimensionless numbers. Here we used the values of 0.4520 nm (0.4970 nm) for the equilibrium lattice parameter of GaN (InN). Eq. (5) represents, to first order in x and ε, the dependence of the LO frequency of the strained InGaN film. However, Eq. (5) does not allow to determine the deformation potentials (or rather the combination of those that define the parameter b) of the InGaN (or even of the end binaries GaN and InN). These parameters were measured for several group IV and II–V semiconductors, and the collected data for those is listed in Table 2. This table shows that the parameter b does not seem to vary from one material to the other. Hence, we can tentatively use the value for this parameter measured with great precision for the LO phonons of GaAs ($b = -1.119$) by Hünermann et al. [14]. Inserting this value in Eq. (5) we obtain the dashed line of Fig. 4. Hence, we have

Table 2
Experimental values of deformation potential constants p and q (divided by ω_0^2) obtained for different zinc-blende materials

	$\frac{p}{2\omega_0^2}$	$\frac{q}{2\omega_0^2}$	α	b	Ref.
GaAs LO-phonon	−0.563	−0.813	0.9010	−1.119	[13]
Ge TO-phonon	−0.737	−0.967	0.7547	−1.204	[14]
GaAs TO-phonon	−0.833	−0.933	0.9010	−1.116	[14]
GaSb TO-phonon	−0.955	−0.967	0.9129	−1.476	[14]
InAs TO-phonon	−0.470	−1.040	1.0873	−1.569	[14]
Si	−0.693	−1.003	0.7704	−1.472	[15]

Values of α and b are calculated by Eqs. (4).

two relevant straight lines in this figure: the full line, representing the dependence of the LO phonon frequency of the unstrained layer on the In molar fraction {Eq. (1)} and the dotted line which is our best estimate for this dependence of the fully strained InGaN layer. If films are fully relaxed, their LO phonon frequencies should fall around the lower (full) line, while those of the fully strained film should fall around the upper (dashed) line. Our data is represented in this figure by full triangles for samples grown on GaAs substrates and full circles for those grown on SiC substrates. This data shows that the former fall around the totally relaxed line (with the exception of sample A5, which is anomalous in many ways), while the latter fall around the fully strained line. This is in consonance with the XRD results (one but last column in Table 1). The only discrepancy between Raman and XRD data is sample B5 ($x = 0.171$ on SiC), which appears as partially relaxed in the Raman data and fully strained in the XRD results. We are not sure why this discrepancy arises, but the good agreement of the other samples grown on SiC with the theoretical Raman line for strained material led us to believe that some strain relaxation is indeed present in this sample, and this amount of relaxation is better registered by the Raman result. In any case, the fact that the samples grown on SiC are close to the fully strained situation while those grown on GaAs are not maybe a reflection of the better crystallinity of the GaN buffer on SiC substrates, as shown by the (I_{TO}/I_{LO}) ratios on their Raman spectra. On the other hand, stress relaxation in the samples grown on GaAs substrates is almost certainly aided by the fact that the alloy layers grown on these substrates are thicker than those grown on SiC substrates (see Table 1).

4. Conclusions

Plasma-assisted MBE was used to obtain epilayers of c-$In_xGa_{1-x}N$/GaN on two types of substrates: (0 0 1) GaAs and (0 0 1) 3C-SiC. The crystalline quality and state of strain in these films were assessed by performing Raman scattering and X-ray diffraction experiments. The results of these studies show that films grown on SiC substrates have better crystalline quality and are better matched to the underlying GaN buffer layer.

Acknowledgements

The authors are thankful to Fundação de Amparo à Pesquisa do Estado de São Paulo (FAPESP, Brazil) and Conselho Nacional de Desenvolvimento Científico e Tecnológico (CNPq-Brazil) for funding in the form of research grants and fellowships. Financial support is gratefully acknowledged to Deutsche Forschungsgemeinschaft (DFG) and the German-Brazilian academic exchange program of DAAD-PROBRAL. Finally we would like to thank Dr. H. Nagasawa and Dr. M. Abe for supplying the 3C-SiC substrates.

References

[1] F.B. Naranjo, S. Fernandez, Ma.A. Sanchez-Garcia, F. Calle, E. Calleja, Appl. Phys. Lett. 80 (12) (2002) 2198.
[2] S.F. Chichibu, M. Sugiyama, T. Onuma, T. Kitamura, H. Nakanishi, T. Kuroda, A. Tackeuchi, T. Sota, Y. Ishida, H. Okumura, Appl. Phys. Lett. 79 (26) (2001) 4319.
[3] F. Calle, F.B. Naranjo, S. Fernandez, M.A. Sanchez-Garcia, E. Calleja, E. Munoz, Phys. Stat. Sol. (a) 192 (2) (2002) 277.
[4] E.D. Pierron, D.L. Paker, J.B. Mc' Nelly, J. Appl. Phys. 38 (1967) 4669.
[5] R.C. Powell, N.E. Lee, Y.W. Kim, J.E. Greene, J. Appl. Phys. 73 (1993) 189.
[6] M.E. Sherwin, T.J. Drummond, J. Appl. Phys. 45 (1974) 2650.

[7] D. Schikora, M. Henkeln, D.J. As, K. Lischka, T. Litz, A. Waag, T. Buhrow, F. Hennebergger, Phys. Rev. B 54 (1996) R8381.
[8] U. Köhler, A study of growth and doping of cubic group III nitride structures, Ph.D. Thesis, Universität Paderborn, Germany, 2002, Cuvillier Verlag Göttingen, ISBN 3-89873-883-3.
[9] D.J. As, in: M.O. Manasreh, I.T. Ferguson (Eds.), III-Nitride Semiconductor Materials: Growth, in series: M.O. Manasreh (Series Ed.), Optoelectronic Properties of Semiconductors and Superlattices, vol. 19, Taylor & Francis Books, Inc., New York, 2003, pp. 323–450 (Chapter 9).
[10] B. Schöttker, Molecular beam epitaxy and characterization of doped and undoped cubic GaN layers, Ph.D. Thesis, Universität Paderborn, Germany, 1999, Shaker Verlag, ISBN 3-8265-6626-2.
[11] A. Tabata, J.R. Leite, A.P. Lima, E. Silveira, V. Lemos, T. Frey, D.J. As, D. Schikora, K. Lischka, Appl. Phys. Lett. 75 (1999) 1095.
[12] E. Silveira, A. Tabata, J.R. Leite, R. Trentin, V. Lemos, T. Frey, D.J. As, D. Schikora, K. Lischka, Appl. Phys. Lett. 75 (1999) 3602.
[13] V. Lemos, E. Silveira, J.R. Leite, A. Tabata, R. Trentin, L.M.R. Scolfaro, T. Frey, D.J. As, D. Schikora, K. Lischka, Phys. Rev. Lett. 84 (2000) 3666.
[14] M. Hünermann, W. Richter, J. Saalmüller, E. Anastassakis, Phys. Rev. B 34 (1986) 5381.
[15] F. Cerdeira, C.J. Buchenauer, F.H. Pollak, M. Cardona, Phys. Rev. B 5 (1972) 580.
[16] F. Cerdeira, A. Pinczuk, J.C. Bean, B. Batlogg, A. Wilson, Appl. Phys. Lett. 45 (1984) 1138.
[17] E. Anastassakis, A. Pinczuk, E. Burstein, F. Pollak, M. Cardona, Solid State Commun. 8 (1970) 133.